Automated 3D Visualization of Electron Microscope Tomograms

Chikara Yamashita
Osaka Institute of Technology
1-79-1, Kitayama
Hirakata, Osaka
573-0196, Japan
yamashita@is.oit.ac.jp

Koji Nishio
Osaka Institute of Technology
1-79-1, Kitayama
Hirakata, Osaka
573-0196, Japan
nishio@is.oit.ac.jp

Ken-ichi Kobori
Osaka Institute of Technology
1-79-1, Kitayama
Hirakata, Osaka
573-0196, Japan
kobori@is.oit.ac.jp

ABSTRACT

In this paper, we propose a 3D visualization method for ultra-high voltage electron microscope tomography intended for use with biological samples. The most important process for constructing 3D images from UHVTEM tomograms is the extraction of contours from 2D sliced images. However, automatic extraction of contours is difficult because of typical noise and artifacts. The proposed method automatically extracts contours by the 3D level set method. In general, the result of the extraction with the level set method depends on the definition of initial contours and parameters. These parameters are usually set manually. Our method automatically generates the initial contours and decides the fittest parameters for the level set method. We verify the effectiveness of our method by applying the technique to two types of unicellular organisms, to compare the results of the proposed method with manual extraction. The automated method successfully identified most cell tissues, with the exception of a limitation in the imaging of tubular-shaped cell structures.

Keywords

Electron microscope tomography, level set method, visualization, segmentation, contour extraction.

1. INTRODUCTION

Ultra-high voltage transmission electron microscopy (UHVTEM) has become a major contribution to medial imaging, because it permits the examination of intracellular structures, which are difficult to examine by conventional X-rays, computed tomography (CT), and magnetic resonance imaging (MRI) techniques [Joa06].

Three-dimensional visualization method can be classified into volume rendering and surface rendering. We use surface rendering to observe object surface. It is possible to extract the three-dimensional structure of cellular structures from UHVTEM data; however, 3D contours are difficult to generate automatically because of noise and artifacts in the data. The traditional approach for generating 3D contours of cellular structures traces the structures on successive two-dimensional slices of a three-dimensional reconstruction. Many hours are required, when the number of sliced images increases.

Our proposed method automatically extracts 3D contours using the level set method [Set99] [Sta03]. Generally, the extraction with the level set method requires the definition of the initial contours and the fittest parameters, which are difficult to define manually. The proposed method automatically generates the initial contours and decides the fittest parameters, thus expediting the process of 3D contour generation. We expect that this refinement of the level set method will facilitate the analysis and recognition of cell pathologies, with applications in a broad spectrum of biomedical disciplines.

2. FEATURES OF ULTRA-HIGH VOLTAGE ELECTRON MICROSCOPE TOMOGRAMS

Ultra-high voltage Electron microscope tomograms are generated by UHVTEM images, obtained on samples with thicknesses in the range of 0.1–10 μm. These thicknesses are sufficient to encompass the size of cell organelles and to permit the quantitative analysis of variations in shape and organization of pathological structures. One of the requirements of

the UHVTEM image is that the missing domain is minimized to enhance the precision of tomographic processing.

A transmitted image is obtained by inclining the sample irradiate the transmitted beam. A missing domain occurs in the resulting image because of mechanical limitations related to rotation of the sample. For example, the reconstructed image in Figure 1(a) reveals decreased resolution in the direction of the missing domain, indicated by the blurred, dim region. Also, the gold particles used in Ultra-High voltage electron microscopy for image alignment and registration appear as granular lines in UHVTEM tomograms; see Figure 1(b).

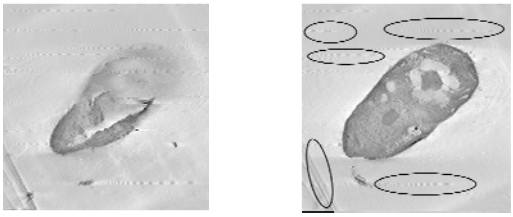

(a) **(b)**

Figure 1. Typical noise in ultra-high voltage electron microscope tomograms: (a) Blurred region reflects low S:N ratios; **(b) Ellipses identify shadows of gold particles.**

3. LEVEL SET METHOD

The level set method is commonly used in medical imaging because it successfully extracts blurred contours [Tak03] [Yos05]. The method is considered an active contour model because it allows topological change. The algorithm extracts contours based on a boundary condition where a region becomes a zero value in high-dimension function. The user defines an initial contour and the level set function which is decided from the initial contour. The algorithm then updates the level set function by solving partial differential equation. The image processing is complete when the variation in the level set function falls below a certain threshold value.

One problem with the level set method is that errors are accumulated at each update of the level set function, causing instabilities in the solution. To achieve a stable solution, the function must be "re-initialized", however, the processing cost of re-initialization is high [Cat03] [Chu05] and various faster methods have been introduced. In our proposed model we use the method of references [Chu05] which is a level set method without re-initialization. In the method of references, the update level set function φ is

$$\phi_{t+1} = \phi_t + rF(\phi) \quad (1)$$

where

$$F(\phi) = \mu \mathrm{P}(\phi) + \lambda L_g(\phi) + \nu A_g(\phi) \quad (2)$$

F is the speed function (the sum of the internal and external energies), r is the weight of the speed function, P is the internal energy function (the effect of re-initialization at the time of the update of the level set function is included), L_g gives the length of the zero isosurface of φ, A_g is introduced to accelerate the update of the level set function,

μ is the weight of the internal energy function, and λ and ν are the weights of the external energy function; if ν is positive, a contour moves in the shrinking direction; otherwise, a contour moves in the expanding direction.

In the level set method, values for the parameters of the level set function are set by experience, usually requiring a number of trials to establish values that give a suitable solution. The model proposed here eliminates these trials by establishing the parameters automatically.

4. 3D VISUALIZATION METHOD

In general, the technique of 3D visualization relies upon laminating the contours of 2D sliced images. When extracting a contour manually, the top and bottom images are established as references. In our proposed automated protocol, the top and bottom images are inputs to the three-dimensional level set method. The level set method requires the input of an initial contour; however, this contour is difficult to set manually. The initial parameters of the level set parameter are also difficult to set, because of the number and variety of cellular structures often embedded in a tomographic image. The proposed automated model sets the initial contour and level set parameters according to procedures in Figure 2.

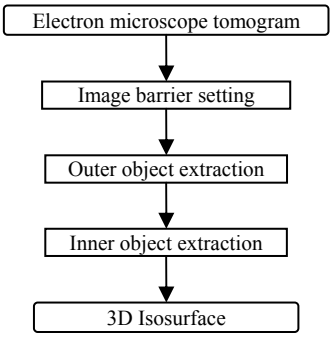

Figure 2. Overview of the proposed automated method.

Step 1) To reduce the influence of the missing domain that is characteristic of ultra-high voltage electron microscope images, an image barrier is set for volume data. The image barrier is discussed in Section 4.3.

Step 2) Extract the contour of outer object using the three-dimensional level set method.

Step 3) Extract the contour of inter object using the three-dimensional level set method.

Step 4) Step 3 is repeated as many times as necessary for each of the varieties of cellular tissue.

Step 5) Isosurfaces are generated using Marching Cubes [Wil87] for the results provided by Steps 2 and 3.

In addition, the proposed method automatically sets an initial contour and parameters for the level set method based on a reference region, as discussed in Section 4.2.

4.1 Definition of tissue boundaries

In order to reduce the processing time in samples with a variety of cell tissue types, the proposed method extracts the contour border of the outer tissue structure, and next extracts the contours of inner tissue structures. This hierarchical extraction technique reduces the processing required for calculations. We define structure of the cell group border of the biotissue as "inner tissue", and other contour and inside domain as "outer tissue". Figure 3 shows the relationship between inner tissue and outer tissue.

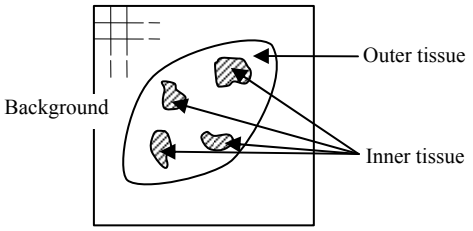

Figure 3. Tissue extraction.

Figure 4 shows the automated procedure to set an initial contour at the border of the outer domain structure. The contour, initially set at the boundary of the image, shrinks to conform to the outer tissue boundary. To set an initial contour on an inner domain structure, the initial contour is defined within the structure, and the contour expands to conform to the inner boundary of the domain.

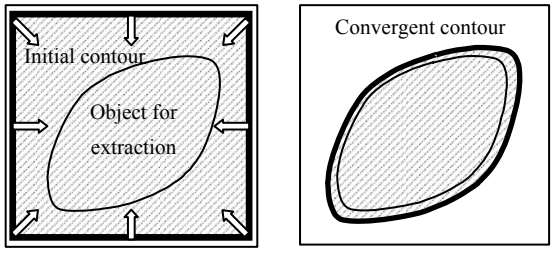

Figure 4. External tissue extraction: (a) Initial contour; (b) Result of extraction

4.2 Automatic initial contour generation

The extraction of the outer boundary of the "outer tissue" is relatively straightforward because the background pixel values are approximately constant. The initial contour for outer tissue can therefore be established either manually or automatically. However, it is difficult to establish an initial contour for inner tissue structures because of the number and variety of associated shapes, textures, brightness intensities, colors, etc. When the inner contours are extracted manually, the operator considers tissues with similar colors as the basis for organization, even if the shape of these structures varies.

Therefore, the proposed method automatically generates the initial contours for inner tissue structures based on color information within the sample. Figure 5 gives an overview of the automated process for initial contour generation.

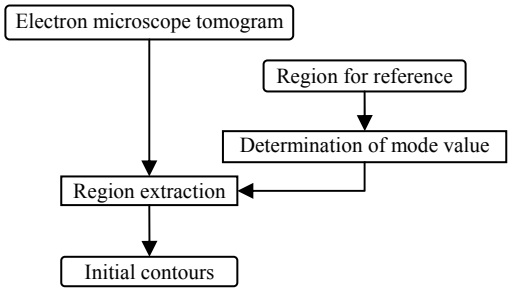

Figure 5. Overview of the automated process of initial contour generation.

Step 1) Choose an image nearly the center of volume data and select a region for contour extraction. Selected region defines the "region for reference"; see Figure 6(a).

Step 2) Determine the mode of brightness values in the region for reference.

Step 3) Determine the extraction range of brightness values for inner tissue

Step 4) To remove noise and artifacts, perform shrinkage processing on the Step 3 result.

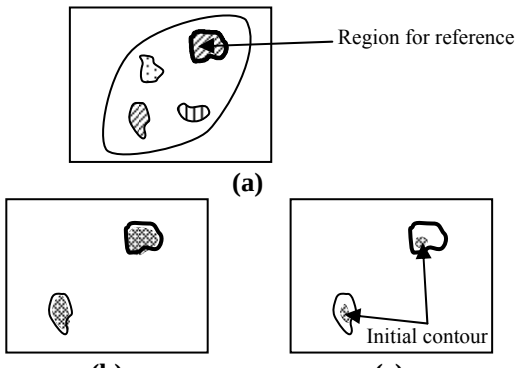

Figure 6. Automatic initial contour generation: (a) Region for reference; (b) Result of region extraction; (c) Initial contour.

If the frequency of brightness values within the inner tissue structure is approximately uniform, then the peak of the distribution defines the mode. The

process chooses a range of brightness values for extraction, and the extraction range encompasses the mode value; see Figure 7.

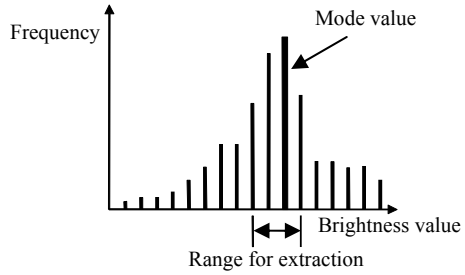

Figure 7. Extraction range.

The extraction range establishes the contrast used by the procedure to define the initial contour. Depending on the extraction range, the procedure may extract pixels that are outward of the actual boundary. In this case, one applies shrinkage processing on the extracted domain in Step 2.

In the proposed method, Steps 2–4 are performed for the cell structures within the outer tissue; repetition of this processing technique extracts the individual elements and establishes the organization framework of the tissue.

4.3 Setting of image barriers

For regions in which a low gradient intensity is included in the image, contours are extracted by the level set method. A contour is defined which extends inside of the cellular structure; see Figure 8(a).

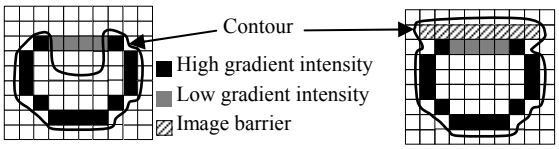

Figure 8. Image barrier (a) before setting and (b) after setting.

In the case of ultra-high voltage electron microscope tomography, missing domains create the region of the low gradient intensities. Missing domains are typically common on upper and lower boundaries. Thus, the application of the three-dimensional level set method may result in contours which extend into the structure. In addition, in the case of a tubular structure oriented in the section direction, a contour may extend into the inner regions of the tissue because the top and bottom boundary surfaces are not distinct. Therefore, the proposed method sets a barrier for the contour by defining the boundary of the structure (Figure 8(b)). This barrier is defined as an "image barrier."

The image barrier is set at the top and bottom ends of the domain manually; see Figure 9. The rectangular domain which encloses the cell tissue is included in these images. These images can them be replaced with the original input image.

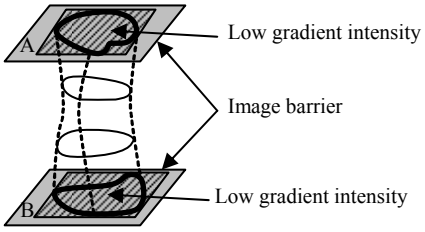

Figure 9. Image barriers.

4.3 Automatic parameter setting

The proposed method sets the parameters for level set method automatically for inner tissue levels. To decrease the processing time, the automated method processes a small domain and translates that domain to the whole image.

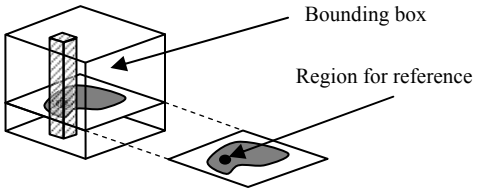

Figure 10. Bounding box generation.

A 3D bounding box is established outside the parcel of inner tissue which includes the region for reference; see Figure 10. The bounding box is elongated in a direction perpendicular to the plane of the region for reference. The initial contour is set using the level set method in this bounding box. The parameters are established when the contour corresponds to the boundary of the region for reference; see Figure 11(a). If the initial contour is inside of the region for reference, the parameters λ and v are increased and the level set method is reapplied; see Figure 11(b). If the initial contour is outside of the region for reference, the parameters λ and v are decreased and the level set method is reapplied; see Figure 11(c).

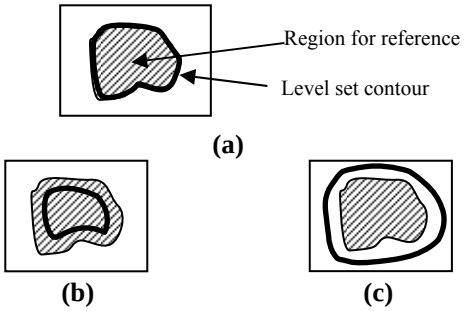

Figure 11. Evaluation of parameters: Fitting the level set contour to the region for reference (a) at the boundary, (b) inside the boundary, and (c) outside the boundary.

5. RESULTS

In our results, we compare the proposed automated method with the manual method of operation. We performed the automatic generation of the initial contour and three-dimensional level set method parameters based on the input of an initial contour.

Figure.12 shows ultra-high voltage electron microscope tomograms used to test the automated method: (a) *Dunaliella parva* (870 × 791 × 146); (b) *Brassica rapa* (512 × 496 × 101).

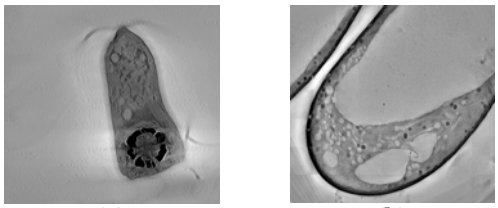

(a) **(b)**

Figure 12. Ultra-high voltage electron microscope tomograms of: (a) *Dunaliella parva*; (b) *Brassica rapa.*

Figures 13 and 14 show the results of 3D visualizations obtained by (a) manual extraction and (b) the proposed automated method. The regions in the visualizations are referred to as outer tissue (regions A and D), granular inner tissue (regions B and E), and "other" inner tissue (regions C and F).

We assessed the effectiveness of the proposed method by evaluating whether contours established by manual extraction are also established by the proposed method. The ratio P of false detections to manually established contours is

$$P = \frac{Negative\_error + Possitive\_error}{V\_manual}. \qquad (3)$$

V_manual is the number of voxels in the region of manual extraction. *Negative_error* is the number of voxels in regions of cellular tissue that the proposed method failed to extract. *Positive_error* is the number of voxels that the proposed method erroneously extracted from regions that were not part of the cellular tissue. P is 0 when the results of the automated and manual extractions are equal.

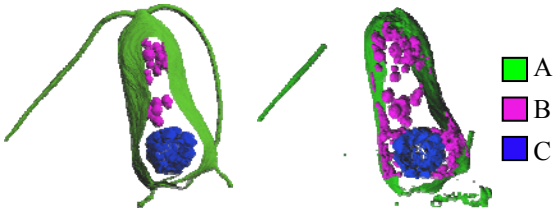

(a) **(b)**

Figure 13. Results for *Dunaliella parva*: (a) Manual extraction; (b) Proposed method.

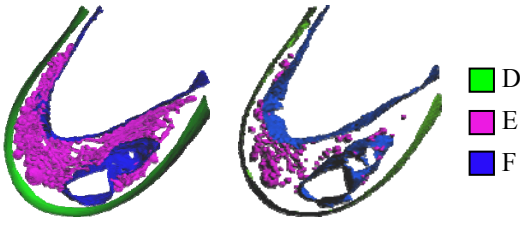

(a) **(b)**

Figure 14. Results for *Brassica rapa*: (a) Manual extraction; (b) Proposed method.

Tables 1 and 2 show the evaluation values and processing time and the number of *V_manual*, *Negative_error* and *Positive_error* voxels, along with their relative contributions (in percentages) to the value of the evaluation parameter P for the 3 regions, in *Dunaliella* and *Brassica*, respectively.

	A	B	C
Evaluation value	0.133	1.464	0.242
Time (hour)	7.0	3.0	1.5
V_manual	13,349,695	449,990	942,446
Negative_error	616,980 4.6%	73,128 16.2%	105,993 11.2%
Positive_error	1,159,883 8.7%	585,851 130.2%	122,052 13.0%

Table 1. Evaluation values and processing time, and voxel values obtained for manually extracted contours, and corresponding errors associated with the automated extraction method; data for *Dunaliella.*

	D	E	F
Evaluation value	0.028	0.910	0.036
Time (hour)	13.2	3.0	15.8
V_manual	14,538,179	890,216	8,466,293
Negative_error	1,240 0.0%	547,500 61.5%	34,231 0.4%
Positive_error	402,573 2.7%	262,993 29.5%	273,441 3.2%

Table 2. Evaluation values and processing time, and Voxel values obtained for manually extracted contours, and corresponding errors associated with the automated extraction method; data for *Brassica.*

Evaluation values obtained for outer tissues (A and D) are less than 0.15 (Tables 1 and 2). Because outer tissues include a large proportion of high gradient intensity regions, which facilitate tomographic processing, it appears that contours can be readily extracted even if the initial contour is set roughly.

The evaluation values for "other" inner tissue regions (C and F) are 0.242 and 0.036 for the 2 trials (Tables 1 and 2). It is thought that initial contour generates cellular tissue in neighborhood. Because ratio these tissue in input tomogram is big.

The evaluation values of granular inner tissues (B and E) are relatively large (1.464 and 0.910; Tables 1 and 2). The *Positive_error* of B is larger than the

value of *V_manual* (Table 1), suggesting that the automatic method extracted an unnecessary domain when the initial contour was generated. Figure 15 shows (a) the original image of *Dunaliella parva* and (b) the initial contours generated by the automatic method (also see Figure 13).

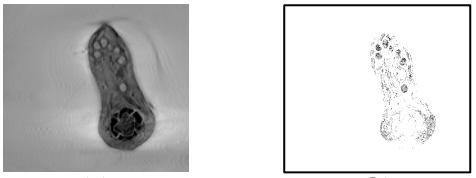

(a) **(b)**

Figure 15. (a) The original image of *Dunaliella parva*, and (b) the initial contours (black pixels) generated by the automated method.

The initial contour extracted for the granular inner tissue domain is represented in Figure 15(b). The level set method extracts a greater region than the manual method, contributing to high *Positive_error* values (130% in *Dunaliella*; Table 1). *Negative_error* values less than 20% of *V_manual* values indicate that the proposed method adequately extracts the spherical cellular tissue. The *Negative_error* for region E is equivalent to 60% of the *V_manual* value (Table 2), probably because this region is a tubular structure.

The capacity of an active contour model to extract objects with vague contours depends on the internal energy. When the internal energy is large, a spherical contour is extracted. However, when the external energy is large, the extraction of contours in inner cell structures with low gradient intensities is problematic. Therefore, the automatic method did not sufficiently expand the contour in the case of the tubular cell tissue, and only an initial contour and the domain of the neighboring cellular tissues were extracted. For this reason, values of the *Negative_error* increased. The extraction of "other" inside tissue contours was apparently unaffected by these considerations.

6. CONCLUSIONS

We propose an automated 3D visualization for ultra-high voltage electron microscope tomograms using the level set method. The method generates an initial contour in the vicinity of manually recognized cell structures. Experimental verification confirmed that the automated method can extract the contours of most cellular tissues, with the exception of tubular-shaped structures. The method may expedite tomographic processing techniques.

Future research will explore the possibility of extracting contours for tubular-shaped tissues.

7. REFERENCES

[Cat03] Cates J.E., Lefohn A.E., Whitaker R.T. GIST: An interactive, GPU-based level set segmentation tool for 3D medical images. *Medical Image Analysis* 8, No. 3, pp. 217-231, 2003.

[Chu05] Chunming, L., Chenyang, X., Changfeng, G., Martin D, Fox. Level set evolution without re-initialization: A new variational formulation. *IEEE International Conference on Computer Vision and Pattern Recognition (CVPR)* 1, pp. 430-436, 2005.

[Joa06] Joachim, F. (ed.) Electron tomography: Methods for three-dimensional visualization of structures in the cell, Springer, Albany, New York, pp. 1-15, 2006.

[Set99] Sethian, J.A. Level set methods and fast marching methods evolving interfaces, in Computational Geometry, Fluid Mechanics, Computer Vision, and Materials Science, Cambridge, England, Cambridge University Press, pp. 214-227, 1999.

[Sta03] Stanley, O., Nikos, P. Geometric level set methods, in Imaging, Vision, and Graphics, Springer-Verlag New York, pp. 1-20, 2003.

[Tak03] Takeshi, H., Akimbo, S., Misato, T., Hidefumi, K. Development of a liver extraction method using a level set method and its performance evaluation. *Journal of Computer Aided Diagnosis of Medical Images* 7, pp. 1-9, 2003.

[Wil87] William E.L., Harvey E.C. Marching cubes: A high resolution 3D surface construction algorithm. *Computer Graphics* 21, No. 4, pp. 163-169, 1987.

[Yos05] Yoshitaka, S., Hideaki, H. Segmentation of medical images using a level-set method. IEICE Technical Report 104, pp. 1-6, 2005.